energies

MDPI

Article

Case Study of an Organic Rankine Cycle (ORC) for Waste Heat Recovery from an Electric Arc Furnace (EAF)

Steven Lecompte [1,2,*], Oyeniyi A. Oyewunmi [3], Christos N. Markides [3], Marija Lazova [1,2], Alihan Kaya [1,2], Martijn van den Broek [1,2] and Michel De Paepe [1,2]

1 Department of Flow, Heat and Combustion Mechanics, Ghent University–UGent, Sint-Pietersnieuwstraat 41, 9000 Gent, Belgium; Marija.Lazova@ugent.be (M.L); Alihan.Kaya@ugent.be (A.K.); Martijn.vandenBroek@ugent.be (M.v.d.V.); Michel.DePaepe@ugent.be (M.D.P.)

2 Flanders Make, the Strategic Research Centre for the Manufacturing Industry, Lommel 3920, Belgium

3 Clean Energy Processes (CEP) Laboratory, Department of Chemical Engineering, Imperial College London, London SW7 2AZ, UK; O.Oyewunmi@imperial.ac.uk (O.A.O.); C.Markides@imperial.ac.uk (C.N.M.)

* Correspondence: steven.lecompte@ugent.be; Tel.: +32-9-264-35-75

Academic Editor: Francesco Calise
Received: 20 March 2017; Accepted: 4 May 2017; Published: 7 May 2017

Abstract: The organic Rankine cycle (ORC) is a mature technology for the conversion of waste heat to electricity. Although many energy intensive industries could benefit significantly from the integration of ORC technology, its current adoption rate is limited. One important reason for this arises from the difficulty of prospective investors and end-users to recognize and, ultimately, realise the potential energy savings from such deployment. In recent years, electric arc furnaces (EAF) have been identified as particularly interesting candidates for the implementation of waste heat recovery projects. Therefore, in this work, the integration of an ORC system into a 100 MWe EAF is investigated. The effect of evaluations based on averaged heat profiles, a steam buffer and optimized ORC architectures is investigated. The results show that it is crucial to take into account the heat profile variations for the typical batch process of an EAF. An optimized subcritical ORC system is found capable of generating a net electrical output of 752 kWe with a steam buffer working at 25 bar. If combined heating is considered, the ORC system can be optimized to generate 521 kWe of electricity, while also delivering 4.52 MW of heat. Finally, an increased power output (by 26% with combined heating, and by 39% without combined heating) can be achieved by using high temperature thermal oil for buffering instead of a steam loop; however, the use of thermal oil in these applications has been until now typically discouraged due to flammability concerns.

Keywords: waste heat recovery; electric arc furnace; organic Rankine cycle; case study

1. Introduction

Vast amounts of thermal energy from various process industries (in the form of flue-gas exhausts, cooling streams, etc.) are currently being wasted by disposal into the environment [1]. These streams are generally considered to be low- to medium-grade (temperature) and as such cannot be efficiently utilized for conversion to power by traditional heat engines such as the steam Rankine cycle. Furthermore, the efficiencies of engines utilizing these waste-heat streams are inherently limited by the low heat-source temperatures. However, the recovery and reuse of these waste-heat streams can significantly improve the overall energy and economic efficiencies of many process plants across a broad range of industries. Thus, the deployment of suitable heat engines capable of efficiently recovering and converting the wasted heat to power has been identified as one of the major pathways towards a high efficiency, sustainable and low-carbon energy future both in the scientific literature [2], and in government and policy-related publications [3].

Various heat-engine technologies have been proposed for the valorization of low-temperature heat [4]. Prime examples include the organic Rankine cycle (ORC) [5], Kalina cycle [6], Goswami cycle [7], and supercritical carbon dioxide (s-CO_2) cycle [8]. These technologies have been deployed successfully for power generation in many diverse applications from domestic [9,10] to industrial [11], and also for the purpose of combined heat and power [12], and even cooling [13]. Although these technologies are more mature, other earlier-stage options are also being currently developed, including various Stirling [14], thermoacoustic [15] and thermofluidic heat engines [16]. In particular, the Non-Inertive-Feedback Thermofluidic Engine (NIFTE) [17,18] and the Up-THERM heat converter [19,20] have been shown to be thermodynamically and economically (due to their small number of moving parts) competitive with established technologies such as ORCs [21].

The ORC, in particular, is an attractive proposition due to its similarity with the well-established steam Rankine-cycle engine, relatively high efficiency compared to the aforementioned low-temperature heat conversion alternatives, and the accompanying wealth of operational and maintenance experience. ORC systems have the design option of employing a number of organic working fluids, ranging from refrigerants to hydrocarbons and siloxanes [22], including working fluid mixtures [23] in order to optimize the heat transfer (and heat recovery) from/to the waste heat source and heat sink [24]. The use of zeotropic mixtures is of particular interest as it can reduce thermodynamic irreversibility, e.g. in the condenser [25]. ORC engines also offer flexibility by featuring a number of potential architectures [26] such as transcritical cycles [27], trilateral cycles [28], partial evaporation cycles [26], and the basic subcritical cycle, to best suit the characteristics of a targeted application heat source and sink. Computer aided molecular design (CAMD) approaches, riding on molecular-based equations of state [29], have also been investigated in a bid to improve the overall heat-to-power conversion efficiency of ORC systems [30].

ORC systems have been studied specifically for waste-heat recovery and conversion in energy intensive industries, where deployed systems span scales from a few kW to tens of MW. More recently, ORCs have also been applied for waste-heat recovery from automobile and marine prime movers such as internal combustion engines [31] and turbocharged diesel engines [32]. They have also been applied for power generation and energy efficiency on offshore oil and gas processing platforms [33], also in combination with wind farms [34]. In addition, over the years, the ORC has also seen applications in the petroleum refining industries from multiple waste-heat sources [35], and in heat recovery from (rotary) kilns in the cement [36] and steel industries [37]. In these systems, an intermediate oil or water loop is employed to recover heat from the waste-heat stream before it is subsequently passed on the working fluid in the cycle.

In the steel industry, which is one of the highest energy and emission intensive sectors, there are multiple avenues for waste heat recovery with ORC systems including from various exhaust gas streams and cooling loops in ore smelting furnaces [38]. Electric arc furnaces (EAF) in particular are considered as important and highly suitable candidates for waste heat recovery projects [39]. The off-gas (i.e., flue-gas) has a high potential for energy recovery. Three different layouts can be conceived to capture this heat: heat exchangers can be placed directly outside the furnace (1600–2000 °C) just after the post combustion (200–900 °C), or they can recover heat by replacing the dry cooler. Inlet gases into the conditioning system just before the stack have temperature values of 80–140 °C. EAF heat recovery systems can be operated via the introduction of an intermediate thermal loop for power generation with an ORC engine. Brandt et al. [40] analyzed a thermal oil operated tube bundle heat exchanger for EAF off-gas heat recovery. They indicate that the main challenge when designing heat exchangers for EAF off-gas is the high variation in temperature and velocity in addition to the fouling. These variations are attributed to the discontinuous operation. They therefore developed a methodology where both the unsteady heat flux and the dust load of the flue gas were considered. This allowed them to design an optimized heat exchanger configuration. Nardin et al. [41] investigated the use of phase change materials (PCM) to smoothen the off-gas temperature. They also proposed to implement cyclones in the actual waste heat recovery unit (WHRU) to overcome

the problem of the high dust content. The WHRU, with the PCM smoothing, resulted in a lower investment cost compared to the design for peak load.

However, the actual integration of an ORC with an EAF has only been investigated and reported in a few studies. Lin et al. [42] investigated the benefit of using an ORC and wood pellet fuel in the steel making process of EAF plants. They however omit examining the waste heat recovery potential of the EAF itself and only consider the reheaters later on in the process.

Turboden implemented the first ORC-based heat recovery plant coupled to an EAF at Elbe-Stahlwerke Feralpi located at Riesa, Germany [43], with a furnace capacity of 133 t/h and a tap-to-tap time of 45 min. The 3-MW electrical output ORC plant exploits a portion of the saturated steam produced and recovers heat from the exhaust gases. The heat recovery system was commissioned in December 2013. Since the EAF is a batch process with high variable heat flow, the inclusion of a steam accumulator was crucial. Compared to thermal oil loops, which work at higher temperatures (280–310 °C), the inclusion of a steam buffer at 26 bar (228–245 °C) implies a reduction in the ORC plant efficiency. The use of thermal oil was however ruled out due to safety reasons (i.e., flammability). The heat recovery process is divided into two main sections. In the first section, the flue gas at a temperature of 1600 °C is cooled by evaporative cooling. Cooling water at boiling point is fed from the steam drum to the cooling loop. This replaces the old cold water cooled ducts. The second section replaces the existing water quench tower (comparable to the dry cooler in the case presented in Section 2). A Waste Heat Steam Generator (WHSG) with vertical tubes was installed. The WHSG includes an evaporator, superheater and economizer. The payback time depends on the use of the steam. Direct use of the steam gives a pay-back time of approximately two to three years, while using the steam for a power generating system has a pay-back time of approximately five to six years.

To the best knowledge of the authors, no single work provides a thorough systematic assessment on the potential of the combined EAF/ORC system. This is also supported by the above literature study wherein either the ORC is investigated as a stand-alone system or the EAF heat recovery units are described in detail. A comprehensive analysis on the potential energy savings for this specific application is therefore missing. As seen from the introduction, the analysis should include the variability of the off-gas, the choice of different intermediate thermal loops and the possibility of novel ORC architectures. This effectively defines the scope of the current work in view of previous studies.

2. The Case Study

Data from an operational 100 MWe electric arc furnace in Belgium is taken for this case study. The layout of the plant is shown in Figure 1. There are two main heat sources available: the low temperature water cooling loops and the exhaust gas after the wet duct. The average available heat of the processes is shown in Figure 2. The temperature in the cooling loops is around 30 °C to 40 °C. For the flue gases, the minimum, maximum and average temperatures and mass flow rates are reported in Table 1. A typical waste heat profile from the flue gas is shown in Figure 3. It is clear that the heat available for recuperation shows a high variation in time. For details about the dynamics, the interested reader is referred to the work of MacRosty and Swartz [44]. For the case under consideration there are two specific constraints. First, the flue gas is available directly before the dry cooler. Secondly, the temperature of the flue gas entering the filters should be between 80 °C and 140 °C. In the remainder of this work, only the flue gases are considered for waste heat recovery due to the very low temperature of the cooling loops and due to the high availability of heat at the flue gas side. The flue gas in this work has been modeled as air considering the high amount of excess air after combustion [45]. Large amounts of air infiltrate trough gaps in the furnace and before the post-combustion chamber.

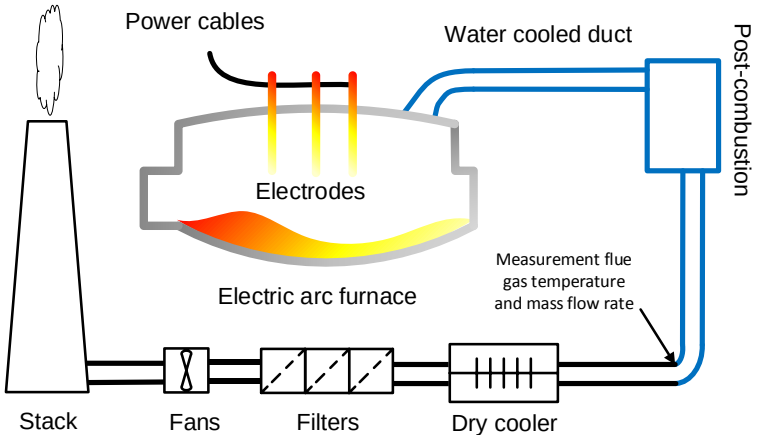

Figure 1. Schematic overview of the electric arc furnace.

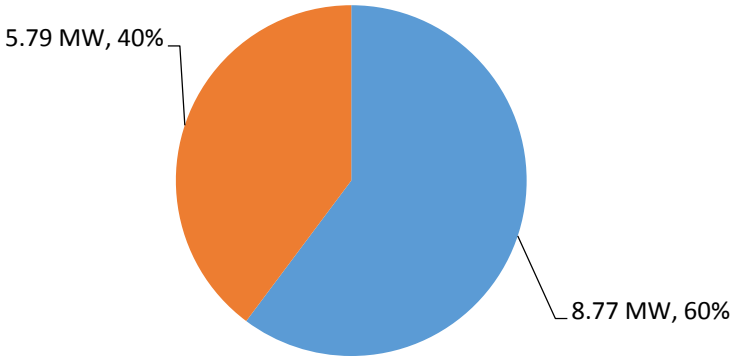

Figure 2. Heat availability averaged over one production run; flue gas reference temperature 90 °C.

Table 1. Characterization of the flue gas heat source.

Value	Maximum	Minimum	Average
Temperature [°C]	578	68	283
Mass flow rate [Nm^3/s]	51.4	0	30.8
Heat transfer rate * [MW]	28.0	0	8.8

Note: * Based on cooling the flue gas to 90 °C.

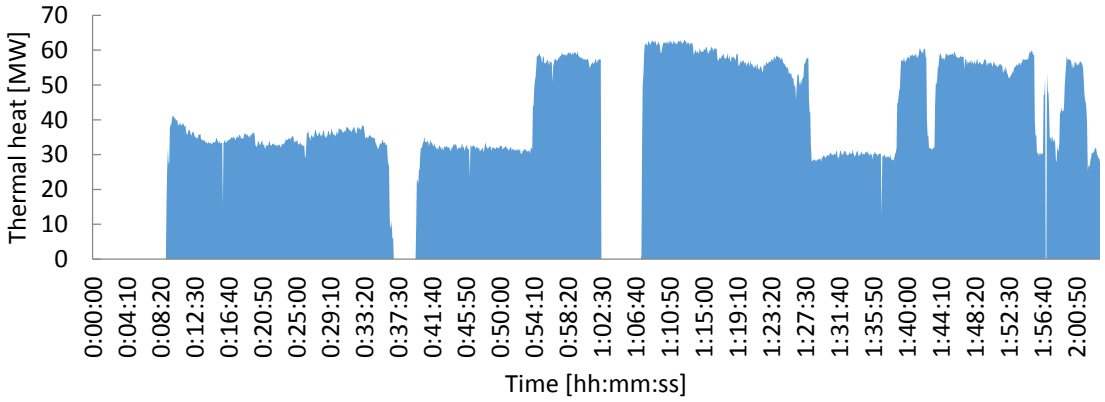

Figure 3. Profile of the available thermal heat (reference cooling temperature of 90 °C).

3. Integrating the Organic Rankine Cycle

ORCs offer the possibility to generate electricity from low capacity and low temperature heat sources. The choice for an ORC to convert heat to power is influenced by the maturity, simplicity and cost-effectiveness of the technology [5].

3.1. ORC Component Layout and Architecture

Conceptually, the ORC is based on the classic (steam) Rankine cycle. The main difference is that instead of water, an alternative organic working fluid is used which has a lower boiling point than water. This is beneficial for low temperature heat recovery as it allows higher efficiencies and power outputs compared to steam Rankine cycles without the need to condense at sub-atmospheric pressures [27]. Also, the volume ratio of turbine outlet and inlet can be reduced compared to water. This allows using smaller and hence cheaper expanders. A reduced specific enthalpy drop permits single-stage turbines instead of the costlier multi-stage machines. Further benefits include: low maintenance, favorable operating pressures and autonomous operation [46]. The benefits associated to ORCs have already been extensively proven by installations in the past [47].

The principle of the basic ORC is given in Figure 4. The key components are the evaporator, expander, condenser and the pump. The hot working fluid leaves the turbine (1) and is condensed in the condenser. The heat from the condensation process is transferred to a cooling loop (7–8) which typically consists of water or air. Subsequently, the condensed working fluid enters (2) the pump and is pressurized (3). Then, the working fluid enters the evaporator and is heated to a superheated state (4). The temperature of the heat carrier (5–6) is thus gradually reduced. The superheated vapor enters the turbine in which it is expanded to provide mechanical power. Next, this cycle is again repeated. The minimum temperature difference between two streams is called the pinch point temperature difference. In the above cycle, there is a pinch point in both the condenser and the evaporator. The numbering scheme introduced in Figure 4 will be used throughout the manuscript. The basic cycle introduced above is called the subcritical cycle (SCORC). This type of cycle is the de facto standard in commercial ORC systems. However, there is ongoing research to further increase the performance of ORCs by considering alternative cycle architectures [26].

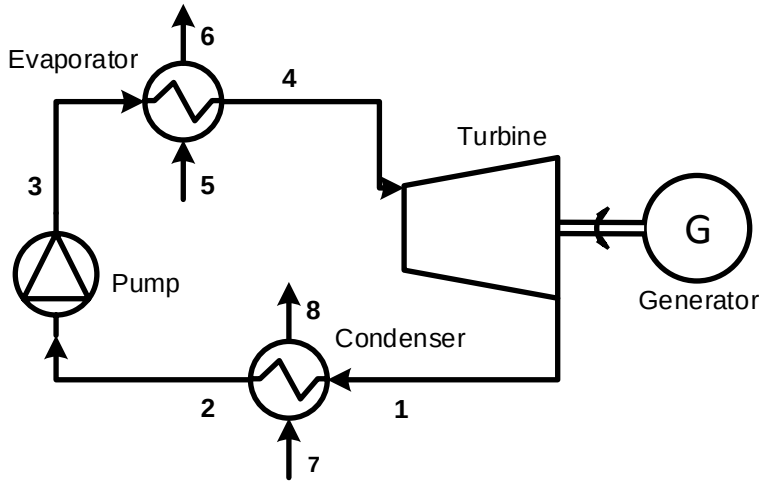

Figure 4. Component layout of the basic organic Rankine cycle (ORC).

3.2. Waste Heat Recovery Options: Steam versus ORC

Excess heat can be recovered and re-used in the process, used for space/water heating onsite, exported "over-the-fence" to nearby plants that have suitable heat sinks in what is known as industrial symbiosis, or to district heating systems. If the waste heat temperature is low, it can be upgraded with

heat pumps to steam for use onsite or to a suitable temperature for the aforementioned uses. If the temperature is high, it can also be used to generate electricity. This is a beneficial choice for the EAF considering that all electricity will be used onsite without any export.

For several applications, there is a choice between both the steam Rankine cycle and the ORC. This decision is not straightforward and is highly case dependent. If there is already a steam loop in the plant, the steam Rankine cycle can be preferred. Typically, for low heat source temperature (<450 °C) and electrical power output (<10 MWe), the ORC technology is favored [48]. In Table 2 we provide comments relating to a direct comparison between the steam Rankine cycle and the ORC.

Table 2. Steam Rankine cycle versus the ORC [27,48].

Criteria	Rankine Cycle	Organic Rankine Cycle
Thermodynamic features	High specific enthalpy drop Superheating needed to avoid droplet erosion	Small specific enthalpy drop No superheating needed
Operation and maintenance	Water treatment required Certified personnel High pressures and temperatures Low condensation pressures	Non-oxidizing working fluids Non-specialized personnel Fully automatic Near-atmospheric condensation
Miscellaneous	Typical for plants >10 MWe and heat input temperatures >450 °C Low off-design flexibility Low performance at part-load	Available for low capacity and low heat-source temperature High off-design flexibility Good performance at part-load

3.3. Selection of the Heat Carrier Loop

In this section, the possibilities of integrating an ORC with a heat carrier loop are discussed. Starting with the low temperature heat from the cooling loops, the ORC working fluid could be pre-heated. However, due to the high mass flow rates and low temperatures this would result in large and expensive heat exchangers. The main reason the heat from the water cooling loops cannot be used is that the condensation temperature of the ORC is not low enough to valorize this heat. Therefore, only the heat of the flue gases is a potential heat source for the ORC system.

The next challenge is the high variance in temperature and mass flow rate of the heat source. ORC systems can operate down to 10% of their nominal load according to Siemens [49] and Turboden [50] (Maxxtec gives a figure of 15%). This means that, without thermal buffering, the ORC would need to restart frequently between operations. Considering the time to start up (up to 30 min [51]) this provides an unworkable situation. Therefore, integration of an intermediate thermal circuit, which can act as buffer, is crucial for the application under consideration. The possible heat carrier options are compared in Table 3. Thermal oil loops are normally not considered in the steel industry, but in order to assess the possible performance benefit, an extra calculation was done in Section 4.4. Two options thus remain: the pressurized hot water loop and the saturated steam loop. Pressurized hot water loops are found in waste incinerators [52] or the steel industry [53]. Steam loops are also found frequently in industry. An additional benefit of steam loops is the possibility to install steam accumulators to efficiently buffer heat. Therefore, the steam loop was selected for further analysis.

Table 3. Possible heat carriers.

Thermal Oil Loop	Pressurized Hot Water Loop	Saturated Steam Loop
High temperatures (<~400 °C)	Low temperatures (<~200 °C)	Medium temperatures (<~300 °C)
High reliability	Simple technical design	Complex technical design
Flammable substances	-	Certified personnel necessary

3.4. Cases under Investigation

Five distinct cases are investigated in this work, which are summarized in Table 4. In the first case (Case 1), the heat profile is simplified by using average values for the temperature and mass flow rate. The cycle is optimized (to maximize the net power output) without any constraints on the evaporation

pressure or the level of superheating. The resulting cycle can thus be: a subcritical ORC (SCORC, i.e., a cycle with superheating), a transcritical ORC (TCORC, i.e., a cycle with evaporation pressure and temperature above the critical point), or a partial evaporation ORC (PEORC, i.e., a cycle with the turbine inlet conditions between saturated liquid and saturated vapor). Details about the different cycle architectures can be found in the work of Lecompte et al. [26]. In the next case (Case 2), an additional constraint is added, such that instead of allowing novel cycle architectures, the ORC is constrained to the commercially available subcritical type. The working parameters of the ORC are optimized as before. Subsequently, in Case 3 an intermediate steam loop at 26 bar (the same value as for the Elbe-Stahlwerke Feralpi plant [43]) is added, which provides the opportunity to buffer heat. In this way, the ORC can operate at steady conditions and the risk of hotspots, e.g., in a directly heated evaporator, is reduced. The ORC is again optimized to operate with the intermediate heat loop. In the fourth case (Case 4), the actual time-varying heat source profiles are introduced corresponding to a single batch process. Finally, in the last case (Case 5) the intermediate steam pressure and ORC operating parameters are optimized. The working fluid is MDM in all cases, which is frequently reported in the literature as a good working fluid for the application considered here [54]. Siloxanes, like MDM, have a low toxicity, low flammability and have a high thermal stability [55]. Furthermore, MDM has a high molecular weight (236.5 kg/kmol) which has a positive impact on the turbine efficiency [56]. The low critical pressure (14.15 bar) results in a favorable evaporator pressure. Lastly, the high critical temperature (290.9 °C) allows capturing the heat with low exergy losses during heat transfer [26]. Further, it is known that Turboden and Maxxtec operate several of their ORCs with MDM [57].

Table 4. Description of the five cases under investigation.

Case	Description
1	No restriction on ORC cycle type, time averaged heat source input values
2	+ Cycle restricted to SCORC operation
3	+ Introduction of an intermediate steam loop
4	+ Use of time dependent heat source profiles as input
5	+ Optimization of operating parameters cycle and steam loop

The five different cases are investigated both for a system with and without combined heating. The system without combined heating directly rejects the available heat at the ORC condenser to the ambient. For the system with combined heating, the condenser is cooled with a high temperature water loop. This high temperature water loop (90–70 °C) can in turn be used to heat buildings.

4. Simulation Results and Discussion

4.1. Boundary Conditions and Model

From a thermodynamic viewpoint, the configuration analyzed with the assumptions made and listed in Table 5 is similar to that of Elbe-Stahlwerke and a similar working fluid condensate temperature (T_2) is obtained.

Table 5. Simulation boundary conditions and assumptions.

Variable	Value
Working fluid	MDM
T_7 [°C]	26 (or 70 with combined heating)
T_8 [°C]	46 (or 90 with combined heating)
Minimum PPTD evaporator [°C]	5 (or higher to keep T_6 >90 °C)
Minimum PPTD condenser [°C]	5
Isentropic efficiency pump [-]	0.70
Isentropic efficiency turbine [-]	0.80

The minimum evaporator pinch point temperature difference is varied in order to keep the flue gas temperature above 90 °C. The results of the simulations are summarized in Table 6. The modelling and optimization approach has been extensively described in previous work by the authors [58]. In this modeling scheme, the power input of the auxiliary equipment (fans, pumps of the cooling loop, etc.) is not considered. Thermophysical data is taken from CoolProp [59].

Table 6. Summary of the ORC simulation results with and without combined heating.

Variable	Value	
Combined heating	Without combined heating	With combined heating
Case 1: PEORC		
Thermal power input [MW]	7.47	7.38
Net power output [MWe]	1.130	0.897
Thermal power output [MW]	0	6.49
Thermal efficiency ORC [%]	13.4	12.2
Mass flow rate cooling water [kg/s]	84.3	77.3
Case 2: SCORC		
Thermal power input [MW]	7.48	7.40
Net power output [MWe]	0.989	0.821
Thermal power output [MW]	0	6.58
Thermal efficiency ORC [%]	13.3	11.1
Mass flow rate cooling water [kg/s]	86.2	78.4
Case 3: SCORC + steam loop		
Thermal power input [MW]	2.79	2.79
Net power output [MWe]	0.380	0.274
Thermal power output [MW]	0	2.52
Thermal efficiency ORC [%]	13.6	9.8
Mass flow rate cooling water [kg/s]	50.1	29
Case 4: SCORC + steam loop + variable heat		
Averaged thermal power input [MW]	5.03	5.03
Averaged net power output [MWe]	0.686	0.494
Thermal power output [MW]	0	4.54
Averaged thermal efficiency ORC [%]	13.6	9.8
Averaged mass flow rate cooling water [kg/s]	50.1	52.3
Case 5: SCORC + steam loop + variable heat + optimized		
Averaged thermal power input [MW]	5.43	5.04
Averaged net power output [MWe]	0.752	0.521
Thermal power output [MW]	0	4.52
Averaged thermal efficiency ORC [%]	13.9	10.3
Averaged mass flow rate cooling water [kg/s]	53.9	52.1

4.2. Simulation Results for the Five Investigated Cases

An overview of the results for the five cases is presented in Table 6. For Case 1, evaluations are performed based on the average values in Table 1. The temperature at the inlet (T_5) is 283 °C and the mass flow rate is 37.7 kg/s. No intermediate steam loop is considered. The *T-s* diagram of the ORC corresponding with maximum power output is given in Figure 5a. The resulting net power output is 1130 kWe. The optimal cycle that emerges in this case is the partial evaporation

ORC (PEORC), although it should be stated that this result relies on the expander achieving a stated isentropic efficiency value of 80% while expanding the working fluid inside the two-phase region.

Nevertheless, PEORCs are not commercially available. Therefore, the constraint is added in Case 2 that the cycle type should correspond to a subcritical ORC (SCORC), with the working fluid being in the saturated or superheated vapor state at the expander inlet. The *T-s* diagram of the optimized cycle under this imposed constraint is shown in Figure 5b. The net power output is reduced from 1130 kWe (Case 1) to 989 kWe which corresponds with a relative decrease of 12.6%. The higher net power output from a PEORC is also confirmed in literature; in these temperature ranges, the expected increase would be around 10% [58]. Again, care should be taken with these results, as the same pump and expander efficiencies are assumed for both the SCORC and PEORC cycle architectures.

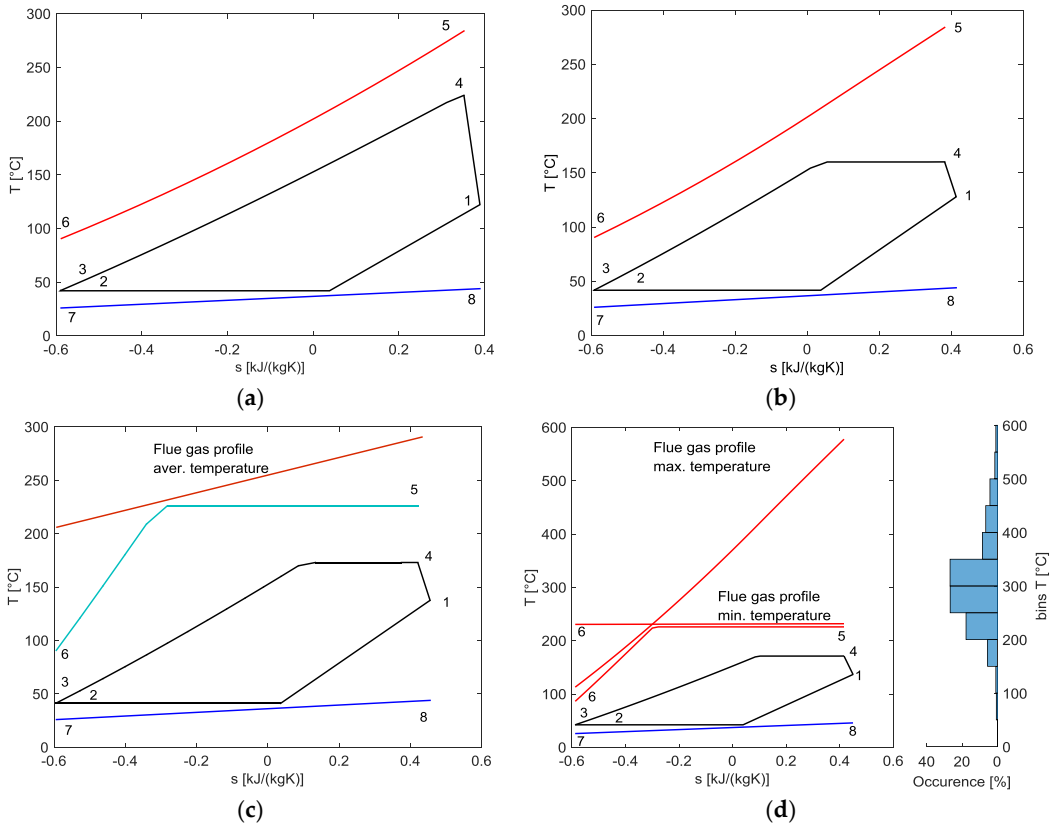

Figure 5. *T-s* diagram without combined heating of (**a**) Case 1 (partial evaporation organic Rankine cycle [PEORC]); (**b**) Case 2 (subcritical ORC); (**c**) Case 3 (subcritical ORC with steam loop); and (**d**) Case 4 (subcritical ORC with steam loop and varying heat input).

Next, an intermediate steam loop is introduced in Case 3. Steam at 26 bar and 230 °C enters the ORC system. These are the same values as for the Elbe-Stahlwerke Feralpi case (see Ref. 41). The steam is condensed and subcooled to 90 °C. The minimum pinch point temperature difference between the flue gas and the intermediate steam loops is fixed at 5 °C. The net power output in this case is further reduced to 381 kWe. In contrast, the thermal efficiency of the ORC only shows a minor change. The large reduction in net power output is attributed to the mismatch between the steam loop and the flue gas. As such, the flue gas exit temperature also rises above 90 °C. The results in a *T-s* diagram are shown in Figure 5c. Note that with higher inlet temperatures the pinch point can shift to the inlet of the steam loop and thus more heat can be transferred.

Therefore, a further analysis was undertaken (Case 4) with time varying inputs of the real heat source profiles. It is assumed that a sufficiently large steam accumulator is present, such that the steam pressure of the intermediate loop can be assumed to be constant in time. The resulting *T-s* diagram is

shown in Figure 5d. The extremes of the flue gas heat profile can easily be identified. The temperature distribution plot furthermore shows that much of the time the temperature of the waste heat is larger than the average value. The total time averaged thermal input is now 5.03 MW. The resulting time averaged net power output is 686 kWe.

In the final and most comprehensive step of Case 5, both the pressure of the intermediate steam loop and the ORC operating parameters are optimized. The results of the optimization are presented in Table 7. The time averaged (net) power output is increased by 9.7% to 752 kWe relative to Case 4 where the steam pressure is not optimized. There is now a slight superheating of roughly 6 °C to attain the maximum net power output. Furthermore, the optimized steam pressure (25 bar) is close to the values of the Elbe-Stahlwerke case (26 bar). Figure 6 shows the instantaneous steam flow rate generated from the waste heat stream. Large variations can be seen during a single batch process, with the steam flow rate varying from 0 to 10.8 kg/s. This plot can be used to size the thermal capacity of the steam buffer to allow a constant time averaged steam flow rate to the ORC of 2.1 kg/s. For all the cases presented, the ORC condensation pressure was around 11.3 mbar.

Table 7. Optimal operating parameters for Case 5.

Variable	Value	
Combined heating	Without combined heating	With combined heating
Pressure steam loop (MPa)	2.50	2.63
Evaporation pressure ORC [kPa]	195	263
Superheat ORC [°C]	5.6	4.9

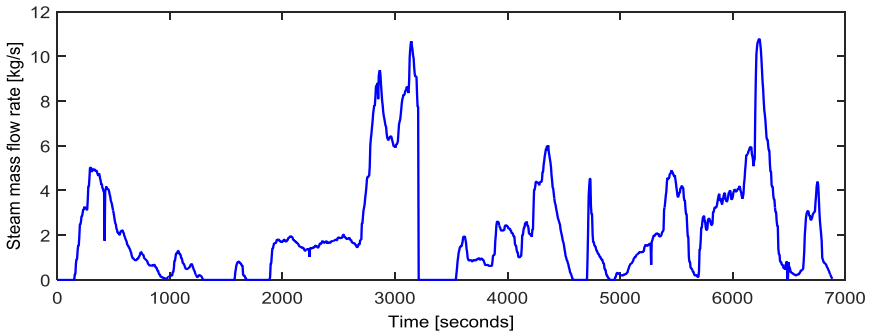

Figure 6. Instantaneous steam flow rate to buffer vessel for a single batch process in Case 5.

4.3. Comparison of Cases with and without Combined Heating

An additional energy benefit and revenue stream can be generated by using the cooling water of the ORC condenser in the proposed setup for space or water heating, although the increased temperature of the cooling loop (90–70 °C) will also lead to an increase in the condensation temperature and a decrease in the thermal efficiency of the ORC system. The results of calculations relating to this possibility are given in Table 6, and the optimized cycle parameters can be found in Table 7. The same five cases discussed above are considered.

It emerges that both the condenser and evaporator will be substantially larger in the case of combined heat provision, due to the decrease in average temperature difference between the different streams. A detailed financial analysis would be necessary for a complete appraisal of the different possibilities; this is however out of the scope of the present work.

The highest power output is again found for the PEORC (Case 1) and amounts to 897 kWe, and the heat to power ratio is 7.22. The corresponding *T-s* diagram can be found in Figure 7a. The net electricity output decreases by 20.7% compared to the situation without combined heating. While there is a noticeable decrease in electricity generated, there is also a vast amount of heat (6.48 MW) which can be used on-site for heating or which can be fed to a district heating network. The practice of

combined heating, however, also leads to lower thermal efficiencies, which is to be expected because of the decrease in the average temperature difference across the ORC.

The difference in thermal power output between Case 1 and Case 2 is rather small (<100 kW). Also, the decrease in net electricity output is low. This is a specific result which has been generalized in previous work [58]. If there is a restriction on the condenser temperature, alternative cycles like the PEORC show an overall lower performance benefit. The *T-s* diagram is given in Figure 7b.

When considering an intermediate steam loop (Case 3), there is a significant reduction in the thermal power going into the ORC, as can be seen in Figure 7c. As a consequence, both the net generated electricity and the thermal power output are dramatically reduced, by 61.7% and 66.6% respectively, compared to Case 2. When considering variable temperature profiles (Case 4), more heat can be transferred to the system (see Figure 7d). As a consequence, the net electricity output and the thermal power output increase again to 494 kWe and 5.03 MW, respectively.

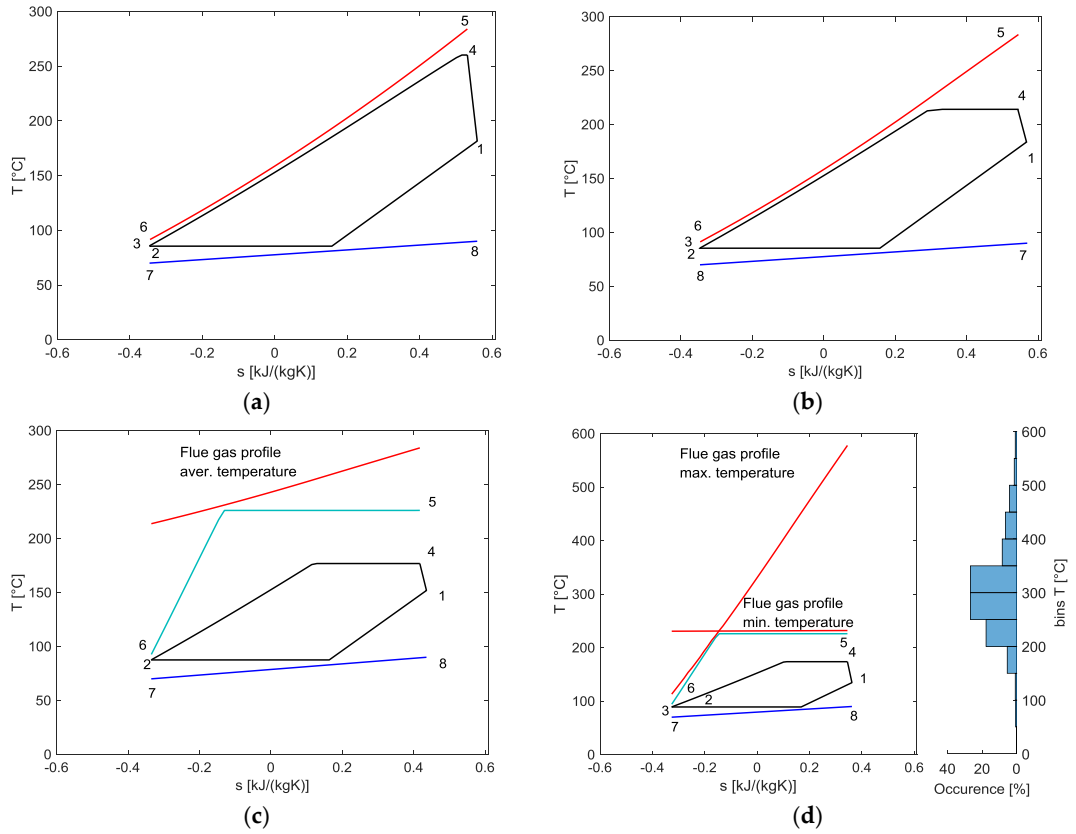

Figure 7. *T-s* diagram with combined heating of (**a**) Case 1 (PEORC); (**b**) Case 2 (subcritical ORC); (**c**) Case 3 (subcritical ORC with steam loop); and (**d**) Case 4 (subcritical ORC with steam loop and varying heat input.

Finally, in Case 5, a system is presented wherein both the pressure of the intermediate steam loop and the ORC operating parameters are optimized. The final ratio of thermal power output to net electricity output is 9.68 with an average net electricity output of 521 kWe.

For all the cases presented in this section, the condensation pressure is around 0.1119 bar. A comprehensive overview of the net power output in all cases is provided in Figure 8, while the heat available for heating in a combined heat and power scenario is indicated in Figure 9.

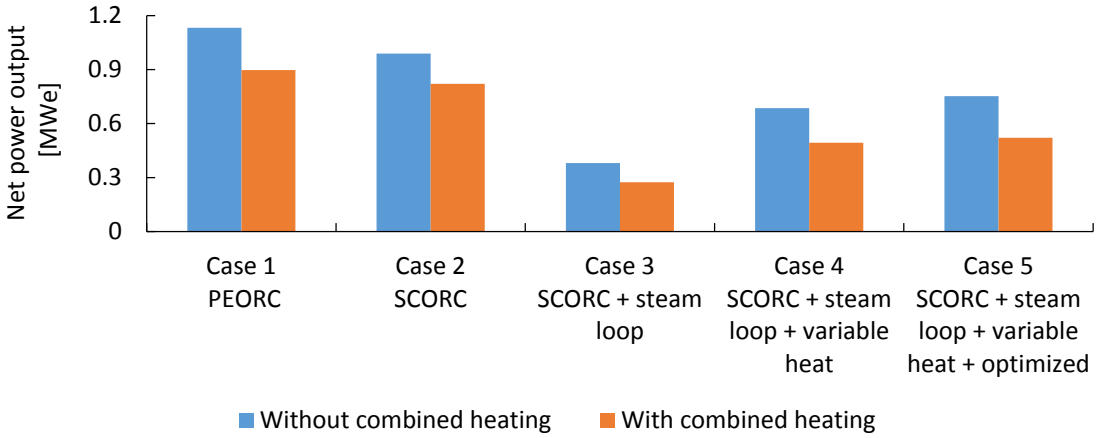

Figure 8. Net power output for the different cases under investigation.

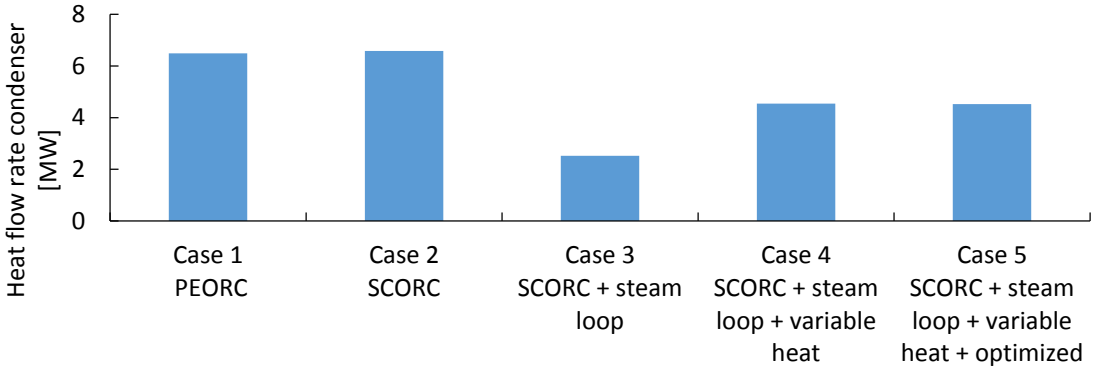

Figure 9. Heat available for combined heating.

4.4. Intermediate Steam Loop versus Thermal Oil Loop

In an extension to the approach presented above, an ORC system with an intermediate thermal oil loop instead of a steam loop was investigated. Thermal oil, Therminol VP-1, was chosen for this investigation, which is an ultra-high temperature synthetic heat transfer fluid designed to meet particularly demanding requirements. Its maximum bulk use temperature is 400 °C. It is also used in concentrated solar power applications [60]. The minimum pinch point temperature difference between the heat carrier and the intermediate oil loop in this case is set to 5 °C. Again, the variability of the waste heat profiles is taken into account and both the cases with and without combined heating are considered.

Results concerning the optimized outlet temperature of the oil loop, ORC evaporation pressure and ORC superheat are summarized in Table 8. By omitting the isothermal plateau of the steam loop, a better match between the heat profiles can be made allowing for improved performance. Using a thermal oil loop results in an increased power output of 39% and 26% for the system without and with combined heating, respectively, compared to the use of an intermediate steam loop (Case 5), although it is noted that the use of thermal oil is typically ruled out in these applications due to safety reasons (i.e., flammability).

Table 8. Summary of ORC simulation results with thermal oil loop, with/without combined heating.

Variable	Value	
Combined heating	Without combined heating	With combined heating
Evaporation pressure ORC [kPa]	185	247
Temperature oil loop in [°C]	122	147
Temperature oil loop out [°C]	215	229
Superheating ORC [°C]	21.6	22.8
Averaged thermal power input [MW]	7.78	6.70
Averaged thermal power output [MW]	0.00	6.41
Averaged net power output [MWe]	1.050	0.659
Averaged thermal efficiency ORC [%]	13.5	9.8
Averaged mass flow rate cooling water [kg/s]	77.6	69.7

5. Conclusions

In this work, a comprehensive analysis concerning the integration of an organic Rankine cycle (ORC) with an electric arc furnace (EAF) was performed. As the EAF is a batch process with large time variation in available thermal capacity and temperature, it was concluded that buffering of the heat is a necessity for which a steam loop is identified as a straightforward solution.

The subsequent analysis was subdivided into five different cases, and the following conclusions can be drawn from the results. Firstly, the partial evaporation cycle (PEORC) provides performance benefits in line with previous research in the literature, showing approximately a 10% higher power output compared to the SCORC. Secondly, the use of a steam buffer greatly reduces the heat transfer to the ORC due to the additional isothermal plateau of steam, decreasing the ORC power output by up to 61.5%. In addition, the use of time averaged input values is not sufficient to accurately simulate ORC/EAF systems as this gives biased results and, further, the optimal pressure of the steam buffer is 25 bar, which closely resembles the 26 bar found in the Elbe-Stahlwerke Feralpi plant [43].

Additionally, the same system with the integration of a hot water loop (90–70 °C) at the condenser side for combined heating was investigated. The results for the optimized ORC and steam loop indicate an electricity output of 521 kWe, which is a decrease of 30.7% compared to the case without combined heating. However, in this scenario there is also a significant amount of heat (4.52 MW) which can be used on-site for space heating or hot water, or in a heat network.

For completeness, a system with a thermal oil loop instead of a steam loop was also studied. When using high temperature thermal oil for buffering, an increased net electrical power output of 26% and 39% relative to the systems with and without combined heating were found, respectively. These are significant improvements; however, the use of thermal oil in the steel industry is generally discouraged because of safety concerns due to their flammability.

The current work only investigates thermodynamic issues. A full appraisal of the project requires a comprehensive financial analysis. This can either be done directly, by calculating the profit over a time period; or indirectly, by using weighing factors to assess the value of heat and electricity. This will be the scope of future work.

Acknowledgments: The results presented in this paper were obtained within the frame of the IWT SBO- 110006 project The Next Generation organic Rankine cycles (www.orcnext.be), funded by the Institute for the Promotion and Innovation by Science and Technology in Flanders. This financial support is gratefully acknowledged. The case study was provided ENGIE Electrabel in the framework of the 'Value of waste heat' project. This work was supported also by the UK Engineering and Physical Sciences Research Council (EPSRC) (Grant no. EP/P004709/1). Data supporting this publication can be obtained on request from steven.lecompte@ugent.be.

Author Contributions: Steven Lecompte performed the simulations, provided the analysis and helped in writing the manuscript; Oyeniyi A. Oyewunmi wrote the literature section and helped with the analysis; Marija Lazova helped with the analysis; Michel De Paepe, Martijn van den Broek and Christos N. Markides revised the manuscript and provided important recommendations; all authors read and approved the final manuscript.

Conflicts of Interest: The authors declare no conflict of interest.

References

1. Ammar, Y.; Joyce, S.; Norman, R.; Wang, Y.; Roskilly, A.P. Low grade thermal energy sources and uses from the process industry in the UK. *Appl. Energy* **2012**, *89*, 3–20. [CrossRef]
2. Markides, C.N. The role of pumped and waste heat technologies in a high-efficiency sustainable energy future for the UK. *Appl. Therm. Eng.* **2013**, *53*, 197–209. [CrossRef]
3. Element Energy, Ecofys, Imperial College, Stevenson, P. (Larksdown Environmental Services), Hyde, R. (RHEnergy). The potential for recovering and using surplus heat from industry. Final report, department of energy and climate change. Available online: https://www.gov.uk/government/uploads/system/uploads/attachment_data/file/294900/element_energy_et_al_potential_for_recovering_and_using_surplus_heat_from_industry.pdf (accessed on 16 March 2017).
4. Chan, C.W.; Ling-Chin, J.; Roskilly, A.P. A review of chemical heat pumps, thermodynamic cycles and thermal energy storage technologies for low grade heat utilisation. *Appl. Therm. Eng.* **2013**, *50*, 1257–1273. [CrossRef]
5. Quoilin, S.; van den Broek, M.; Declaye, S.; Dewallef, P.; Lemort, V. Techno-economic survey of organic Rankine cycle (ORC) systems. *Renew. Sustain. Energy Rev.* **2013**, *22*, 168–186. [CrossRef]
6. Zhang, X.; He, M.; Zhang, Y. A review of research on the Kalina cycle. *Renew. Sustain. Energy Rev.* **2012**, *16*, 5309–5318. [CrossRef]
7. Goswami, D.Y. Solar thermal power technology: Present status and ideas for the future. *Energy Sources* **1998**, *20*, 137–145. [CrossRef]
8. Akbari, A.D.; Mahmoudi, S.M.S. Thermoeconomic analysis & optimization of the combined supercritical CO_2 (carbon dioxide) recompression Brayton/organic Rankine cycle. *Energy* **2014**, *78*, 501–512.
9. Freeman, J.; Hellgardt, K.; Markides, C.N. An assessment of solar-powered organic Rankine cycle systems for combined heating and power in UK domestic applications. *Appl. Energy* **2015**, *138*, 605–620. [CrossRef]
10. Freeman, J.; Hellgardt, K.; Markides, C.N. Working fluid selection and electrical performance optimisation of a domestic solar-ORC combined heat and power system for year-round operation in the UK. *Appl. Energy* **2017**, *186*, 291–303. [CrossRef]
11. Ibrahim, M.B.; Kovach, R.M. A Kalina cycle application for power generation. *Energy* **1993**, *18*, 961–969. [CrossRef]
12. Markides, C.N. Low-concentration solar-power systems based on organic Rankine cycles for distributed-scale applications: Overview and further developments. *Front. Energy Res.* **2015**, *3*, 47. [CrossRef]
13. Vijayaraghavan, S.; Goswami, D. A combined power and cooling cycle modified to improve resource utilization efficiency using a distillation stage. *Energy* **2006**, *31*, 1177–1196. [CrossRef]
14. Ceperley, P.H. A pistonless Stirling engine—the traveling wave heat engine. *J. Acoust. Soc. Am.* **1979**, *66*, 1508–1513. [CrossRef]
15. Backhaus, S.; Swift, G.W. A thermoacoustic-Stirling heat engine: Detailed study. *J. Acoust. Soc. Am.* **2000**, *107*, 3148–3166. [CrossRef] [PubMed]
16. Markides, C.N.; Smith, T.C.B. A dynamic model for the efficiency optimization of an oscillatory low grade heat engine. *Energy* **2011**, *36*, 6967–6980. [CrossRef]
17. Solanki, R.; Galindo, A.; Markides, C.N. Dynamic modelling of a two-phase thermofluidic oscillator for efficient low grade heat utilization: Effect of fluid inertia. *Appl. Energy* **2012**, *89*, 156–163. [CrossRef]
18. Markides, C.N.; Solanki, R.; Galindo, A. Working fluid selection for a two-phase thermofluidic oscillator: Effect of thermodynamic properties. *Appl. Energy* **2014**, *124*, 167–185. [CrossRef]
19. Oyewunmi, O.A.; Kirmse, C.J.W.; Haslam, A.J.; Müller, E.A.; Markides, C.N. Working-fluid selection and performance investigation of a two-phase single-reciprocating-piston heat-conversion engine. *Appl. Energy* **2017**, *186*, 376–395. [CrossRef]
20. Kirmse, C.J.W.; Oyewunmi, O.A.; Taleb, A.I.; Haslam, A.J.; Markides, C.N. Two-phase single-reciprocating-piston heat conversion engine: Non-linear dynamic modelling. *Appl. Energy* **2017**, *186*, 359–375. [CrossRef]
21. Kirmse, C.J.W.; Oyewunmi, O.A.; Haslam, A.J.; Markides, C.N. Comparison of a novel organic-fluid thermofluidic heat converter and an organic Rankine cycle heat engine. *Energies* **2016**, *9*, 47. [CrossRef]
22. Chen, H.; Goswami, D.Y.; Stefanakos, E.K. A review of thermodynamic cycles and working fluids for the conversion of low-grade heat. *Renew. Sustain. Energy Rev.* **2010**, *14*, 3059–3067. [CrossRef]

23. Oyewunmi, O.A.; Taleb, A.I.; Haslam, A.J.; Markides, C.N. On the use of SAFT-VR Mie for assessing large-glide fluorocarbon working-fluid mixtures in organic Rankine cycles. *Appl. Energy* **2016**, *163*, 263–282. [CrossRef]
24. Oyewunmi, O.A.; Markides, C.N. Thermo-economic and heat transfer optimization of working-fluid mixtures in a low-temperature organic Rankine cycle system. *Energies* **2016**, *9*, 448. [CrossRef]
25. Lecompte, S.; Ameel, B.; Ziviani, D.; van den Broek, M.; De Paepe, M. Exergy analysis of zeotropic mixtures as working fluids in organic Rankine cycles. *Energy Convers. Manag.* **2014**, *85*, 727–739. [CrossRef]
26. Lecompte, S.; Huisseune, H.; van den Broek, M.; Vanslambrouck, B.; De Paepe, M. Review of organic Rankine cycle (ORC) architectures for waste heat recovery. *Renew. Sustain. Energy Rev.* **2015**, *47*, 448–461. [CrossRef]
27. Lecompte, S.; Lemmens, S.; Huisseune, H.; van den Broek, M.; De Paepe, M. Multi-objective thermo-economic optimization strategy for ORCs applied to subcritical and transcritical cycles for waste heat recovery. *Energies* **2015**, *8*, 2714–2741. [CrossRef]
28. Fischer, J. Comparison of trilateral cycles and organic Rankine cycles. *Energy* **2011**, *36*, 6208–6219. [CrossRef]
29. Lampe, M.; Kirmse, C.; Sauer, E.; Stavrou, M.; Gross, J.; Bardow, A. Computer-aided molecular design of ORC working fluids using PC-SAFT. *Comput. Aided Chem. Eng.* **2014**, *34*, 357–362.
30. White, M.T.; Oyewunmi, O.A.; Haslam, A.J.; Markides, C.N. Industrial waste-heat recovery through integrated computer-aided working-fluid and ORC system optimisation using SAFT-γ Mie. *Energy Convers. Manag.* **2017**, In Press. Available online: https://doi.org/10.1016/j.enconman.2017.03.048 (accessed on 25 April 2017).
31. Zhao, M.; Wei, M.; Song, P.; Liu, Z.; Tian, G. Performance evaluation of a diesel engine integrated with ORC system. *Appl. Therm. Eng.* **2017**, *115*, 221–228. [CrossRef]
32. Di Battista, D.; Mauriello, M.; Cipollone, R. Waste heat recovery of an ORC-based power unit in a turbocharged diesel engine propelling a light duty vehicle. *Appl. Energy* **2015**, *152*, 109–120. [CrossRef]
33. Nguyen, T.-V.; Voldsund, M.; Breuhaus, P.; Elmegaard, B. Energy efficiency measures for offshore oil and gas platforms. *Energy* **2016**, *117*, 325–340. [CrossRef]
34. Orlandini, V.; Pierobon, L.; Schløer, S.; De Pascale, A.; Haglind, F. Dynamic performance of a novel offshore power system integrated with a wind farm. *Energy* **2016**, *109*, 236–247. [CrossRef]
35. Yu, H.; Feng, X.; Wang, Y.; Biegler, L.T.; Eason, J. A systematic method to customize an efficient organic Rankine cycle (ORC) to recover waste heat in refineries. *Appl. Energy* **2016**, *179*, 302–315. [CrossRef]
36. Karellas, S.; Leontaritis, A.-D.; Panousis, G.; Bellos, E.; Kakaras, E. Energetic and exergetic analysis of waste heat recovery systems in the cement industry. *Energy* **2013**, *58*, 147–156. [CrossRef]
37. Campana, F.; Bianchi, M.; Branchini, L.; De Pascale, A.; Peretto, A.; Baresi, M.; Fermi, A.; Rossetti, N.; Vescovo, R. ORC waste heat recovery in European energy intensive industries: Energy and GHG savings. *Energy Convers. Manag.* **2013**, *76*, 244–252. [CrossRef]
38. Lazzarin, R.M.; Noro, M. Energy efficiency opportunities in the production process of cast iron foundries: An experience in Italy. *Appl. Therm. Eng.* **2015**, *90*, 509–520. [CrossRef]
39. Sung, T.; Yun, E.; Kim, H.D.; Yoon, S.Y.; Choi, B.S.; Kim, K.; Kim, J.; Jung, Y.B.; Kim, K.C. Performance characteristics of a 200 kW organic Rankine cycle system in a steel processing plant. *Appl. Energy* **2016**, *183*, 623–635. [CrossRef]
40. Brandt, C.; Schüler, N.; Gaderer, M.; Kuckelkorn, J.M. Development of a thermal oil operated waste heat exchanger within the off-gas of an electric arc furnace at steel mills. *Appl. Therm. Eng.* **2014**, *66*, 335–345. [CrossRef]
41. Nardin, G.; Meneghetti, A.; Dal Magro, F.; Benedetti, N. PCM-based energy recovery from electric arc furnaces. *Appl. Energy* **2014**, *136*, 947–955. [CrossRef]
42. Lin, Y.-P.; Wang, W.-H.; Pan, S.-Y.; Ho, C.-C.; Hou, C.-J.; Chiang, P.-C. Environmental impacts and benefits of organic Rankine cycle power generation technology and wood pellet fuel exemplified by electric arc furnace steel industry. *Appl. Energy* **2016**, *183*, 369–379. [CrossRef]
43. Bause, T.; Campana, F.; Filippini, L.; Foresti, A.; Monti, N.; Pelz, T. Cogeneration with ORC at Elbe-Stahlwerke Feralpi EAF Shop. In Proceedings of the Iron & Steel Technology Conference and Exposition, Indianapolis, IN, USA, 5–8 May 2014.
44. MacRosty, R.D.M.; Swartz, C.L.E. Dynamic Modeling of an Industrial Electric Arc Furnace. *Ind. Eng. Chem. Res.* **2005**, *44*, 8067–8083. [CrossRef]
45. Coskun, C.; Oktay, Z.; Ilten, N. A new approach for simplifying the calculation of flue gas specific heat and specific exergy value depending on fuel composition. *Energy* **2009**, *34*, 1898–1902. [CrossRef]

46. Tchanche, B.F.; Lambrinos, G.; Frangoudakis, A.; Papadakis, G. Low-grade heat conversion into power using organic Rankine cycles – A review of various applications. *Renew. Sustain. Energy Rev.* **2011**, *15*, 3963–3679. [CrossRef]
47. Bronicki, L. Short review of the long history of ORC power systems. In Proceedings of the ORC2013, Rotterdam, The Netherlands, 7–8 October 2013.
48. Crook, A.W. *Profiting from Low-Grade Heat*; Institution of Electrical Engineers: Stevenage, Hertfordshire, 1994.
49. Siemens. Fact Sheet: Organic Rankine Cycle. Available online: http://www.energy.siemens.com/nl/pool/hq/power-generation/steam-turbines/orc-technology/Siemens_FactSheet-ORC-Module.pdf (accessed on 1 May 2016).
50. Turboden. Organic Rankine Cycle Technology. Available online: http://www.turboden.eu/en/public/downloads/200-300%20kW.pdf (accessed on 5 April 2016).
51. Uusitalo, A.; Honkatukia, J.; Backman, J.; Nyyssönen, S. Experimental study on charge air heat utilization of large-scale reciprocating engines by means of organic Rankine cycle. *Appl. Therm. Eng.* **2015**, *89*, 209–219. [CrossRef]
52. MIROM. Verbrandingsinstallatie: enkele cijfers. Available online: http://www.mirom.be/verbranding_cijfers.html (accessed on 1 May 2017).
53. David, G.; Michel, F.; Sanchez, L. *Waste Heat Recovery Projects Using Organic Rankine Cycle Technology—Examples of Biogas Engines and Steel Mills Applications*; World Engineers Convention: Geneva, Switzerland, 2011.
54. Fernández, F.J.; Prieto, M.M.; Suárez, I. Thermodynamic analysis of high-temperature regenerative organic Rankine cycles using siloxanes as working fluids. *Energy* **2011**, *36*, 5239–5249. [CrossRef]
55. Bao, J.; Zhao, L. A review of working fluid and expander selections for organic Rankine cycle. *Renew. Sustain. Energy Rev.* **2013**, *24*, 325–342. [CrossRef]
56. Stijepovica, M.Z.; Linke, P.; Papadopoulos, A.I.; Grujic, A.S. On the role of working fluid properties in Organic Rankine Cycle performance. *Appl. Therm. Eng.* **2012**, *36*, 406–413. [CrossRef]
57. Maraver, D.; Royo, J.; Lemort, V.; Quoilin, S. Systematic optimization of subcritical and transcritical organic Rankine cycles (ORCs) constrained by technical parameters in multiple applications. *Appl. Energy* **2014**, *117*, 11–29. [CrossRef]
58. Lecompte, S.; Huisseune, H.; van den Broek, M.; De Paepe, M. Methodical thermodynamic analysis and regression models of organic Rankine cycle architectures for waste heat recovery. *Energy* **2016**, *87*, 60–76. [CrossRef]
59. Bell, I.H.; Wronski, J.; Quoilin, S.; Lemort, V. Pure and pseudo-pure fluid thermophysical property evaluation and the open-source thermophysical property library CoolProp. *Ind. Eng. Chem. Res.* **2014**, *53*, 2498–2508. [CrossRef] [PubMed]
60. Pacheco, J.E.; Showalter, S.K.; Kolb, W.J. Development of a molten-salt thermocline thermal storage system for parabolic trough plants. *J. Sol. Energy Eng.* **2002**, *124*, 153–159. [CrossRef]